



# Synthesis of $Zr_2WP_2O_{12}/ZrO_2$ Composites with Adjustable Thermal Expansion

Zhiping Zhang<sup>1,2</sup>, Weikang Sun<sup>1</sup>, Hongfei Liu<sup>1\*</sup>, Guanhua Xie<sup>2</sup>, Xiaobing Chen<sup>1,2</sup> and Xianghua Zeng<sup>1</sup>

<sup>1</sup> Department of Electrical and Mechanical Engineering, Guangling College, Yangzhou University, Yangzhou, China, <sup>2</sup> School of Physical Science and Technology, Yangzhou University, Yangzhou, China

## OPEN ACCESS

### Edited by:

Jun Chen,  
University of Science and Technology  
Beijing, China

### Reviewed by:

Peng Tong,  
Institute of Solid State Physics, Hefei  
Institutes of Physical Science (CAS),  
China  
Rongjin Huang,  
Technical Institute of Physics and  
Chemistry (CAS), China

### \*Correspondence:

Hongfei Liu  
liuhf@yzu.edu.cn

### Specialty section:

This article was submitted to  
Physical Chemistry and Chemical  
Physics,  
a section of the journal  
Frontiers in Chemistry

Received: 27 September 2017

Accepted: 03 November 2017

Published: 21 November 2017

### Citation:

Zhang Z, Sun W, Liu H, Xie G, Chen X  
and Zeng X (2017) Synthesis of  
 $Zr_2WP_2O_{12}/ZrO_2$  Composites with  
Adjustable Thermal Expansion.  
Front. Chem. 5:105.  
doi: 10.3389/fchem.2017.00105

$Zr_2WP_2O_{12}/ZrO_2$  composites were fabricated by solid state reaction with the goal of tailoring the thermal expansion coefficient. XRD, SEM and TMA were used to investigate the composition, microstructure, and thermal expansion behavior of  $Zr_2WP_2O_{12}/ZrO_2$  composites with different mass ratio. Relative densities of all the resulting  $Zr_2WP_2O_{12}/ZrO_2$  samples were also tested by Archimedes' methods. The obtained  $Zr_2WP_2O_{12}/ZrO_2$  composites were comprised of orthorhombic  $Zr_2WP_2O_{12}$  and monoclinic  $ZrO_2$ . As the increase of the  $Zr_2WP_2O_{12}$ , the relative densities of  $Zr_2WP_2O_{12}/ZrO_2$  ceramic composites increased gradually. The coefficient of thermal expansion of the  $Zr_2WP_2O_{12}/ZrO_2$  composites can be tailored from  $4.1 \times 10^{-6} K^{-1}$  to  $-3.3 \times 10^{-6} K^{-1}$  by changing the content of  $Zr_2WP_2O_{12}$ . The 2:1  $Zr_2WP_2O_{12}/ZrO_2$  specimen shows close to zero thermal expansion from 25 to 700°C with an average linear thermal expansion coefficient of  $-0.09 \times 10^{-6} K^{-1}$ . These adjustable and near zero expansion ceramic composites will have great potential application in many fields.

**Keywords:**  $Zr_2WP_2O_{12}$ ,  $ZrO_2$ , composites, thermal expansion, ceramics

## INTRODUCTION

Lots of materials known to show positive thermal expansion as temperature increase. In contrast, some materials show completely different thermal expansion properties and contract upon heating. This negative thermal expansion (NTE) phenomena has been found in some  $A_2(MO_4)_3$  compounds, where the A cation can be a trivalent main group metal, transition metal, or rare earth element ranging from Lu to Ho, while M corresponds to W or Mo (Sumithra and Umarji, 2004, 2006; Liu H. F. et al., 2012; Liu Q. Q. et al., 2012; Liu et al., 2015). In addition, compounds with aliovalent cations on the A and M site have been reported. For example,  $Zr_2WP_2O_{12}$  has been reported to exhibit strong and stable NTE over a wide temperature range.  $Zr_2WP_2O_{12}$  adopts the orthorhombic  $Sc_2W_3O_{12}$  structure, which consists of  $ZrO_6$  octahedra that share corners with two  $WO_4$  tetrahedra and four  $PO_4$  tetrahedra. Zr-O-W (P) linkages in this structure will lead to the volume contraction due to transverse vibration of bridging oxygen atoms as temperature increase (Isobe et al., 2008, 2009; Cetinkol and Wilkinson, 2009; Tani et al., 2010).

Thermal expansion is an important property of materials, and mismatch in thermal expansion often induces unstable performance or failure of devices in the field of microelectronics, optics and micromachines. To avoid the above problems, control of thermal expansion of materials can be necessary. An easy approach is to mix the NTE material with the positive thermal expansion material in the right proportion.

Most studies describing attempts to synthesize controllable thermal expansion composites mainly focus on  $ZrW_2O_8$  based composites, such as  $ZrW_2O_8/ZrO_2$  (De Buysser et al., 2004; Lommens et al., 2005; Yang et al., 2007; Khazeni et al., 2011; Romao et al., 2015),  $ZrW_2O_8/Cu$  and  $ZrW_2O_8/polyimide$  (Yilmaz, 2002; Sullivan and Lukehart, 2005; Yang et al., 2010; Hu et al., 2014). The coefficient of thermal expansion (CTE) of the composites drops with the increase of the  $ZrW_2O_8$  filler. However, the cubic NTE phase of  $ZrW_2O_8$  is metastable at room temperature, and has to be prepared by rapid quenching after sintering at  $1,200^\circ C$ . Cubic  $ZrW_2O_8$  show a isotropic NTE over a wide temperature range, but a phase transition from  $\alpha$ - $ZrW_2O_8$  to  $\beta$ - $ZrW_2O_8$  occurs around  $160^\circ C$ , which leads to the decrease of CTE. This change in thermal expansion may be disadvantageous for composite design. Moreover, when heated to  $740^\circ C$ ,  $ZrW_2O_8$  decomposes into  $ZrO_2$  and  $WO_3$  (Mary et al., 1996; Banek et al., 2010; Gao et al., 2016). In addition, cubic  $ZrW_2O_8$  undergoes a pressure induced phase transition to an orthorhombic phase with a positive CTE. This transformation has been observed in composites during thermal cycling, and leads to irreproducible thermal expansion behavior (Perottoni and Jornada, 1998; Miao et al., 2004; Varga et al., 2007; Liu et al., 2014).

$Zr_2WP_2O_{12}$  is a new NTE material for use as a filler to adjust the CTE of ceramics, glasses, metals, and polymers. It exhibits a strong NTE over the broadest temperature range (room temperature to its sublimation point of about  $1,600^\circ C$ ). Moreover, it does not suffer from the same limitations as  $ZrW_2O_8$ , as it is thermodynamically stable and does not undergo any phase transformations.

The synthesis and NTE behavior of  $Zr_2WP_2O_{12}$  ceramics have been reported previously (Isobe et al., 2008, 2009; Cetinkol and Wilkinson, 2009; Tani et al., 2010).  $Zr_2WP_2O_{12}$  ceramics show stable NTE with an average linear CET of about  $-5 \times 10^{-6} K^{-1}$ . In addition, the  $Zr_2WP_2O_{12}$  ceramics display excellent mechanical properties (Isobe et al., 2008, 2009; Cetinkol and Wilkinson, 2009).  $ZrO_2$  ceramics and fibers has been widely used in optics, electronics and high temperature fields (Lommens et al., 2005; Yang et al., 2007). In some special occasions,  $ZrO_2$  need to keep precision dimensional stability with the change in temperature, because a mismatch in size among different precision devices can cause some problems. The average linear CTE of  $ZrO_2$  is about  $10 \times 10^{-6} K^{-1}$  from room temperature to  $1,000^\circ C$ . The absolute values of the CTE of  $ZrO_2$  and  $Zr_2WP_2O_{12}$  are thus similar but have opposite signs, suggesting that these materials are good candidates for the preparation of ceramic composites with tunable CTEs. It is beneficial that  $ZrO_2$  does not react with  $Zr_2WP_2O_{12}$  at high temperatures, as it is a starting material in the solid state synthesis of  $Zr_2WP_2O_{12}$ .

A new series of  $Zr_2WP_2O_{12}/ZrO_2$  ceramic composites that are expected to show an adjustable CTE were synthesized by a solid state reaction method. This work is devoted to exploring the effects of mass ratio of  $Zr_2WP_2O_{12}$  and  $ZrO_2$  on the microstructure, density, and CTE values of the  $Zr_2WP_2O_{12}/ZrO_2$  ceramic composites.

**TABLE 1** | Synthesis conditions for  $ZrO_2/Zr_2WP_2O_{12}$  ceramics.

Mass ratio of $Zr_2WP_2O_{12}:ZrO_2$	$m(ZrO_2)/g$	$m(WO_3)/g$	$m(NH_4H_2PO_4)/g$
0:1	10	0	0
1:1	6.99	1.87	1.86
2:1	7.18	2.99	2.97
3:1	6.58	3.36	3.34
4:1	5.18	2.99	2.97
1:0	3.97	3.74	3.71

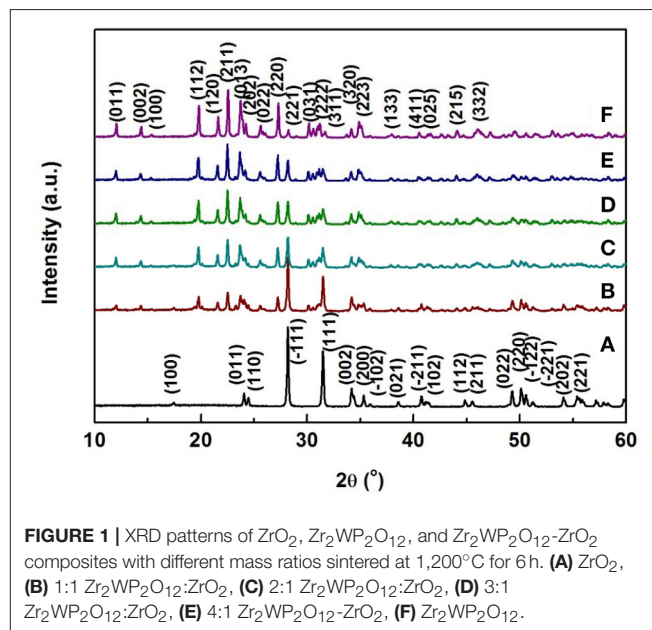


**FIGURE 1** | XRD patterns of  $ZrO_2$ ,  $Zr_2WP_2O_{12}$ , and  $Zr_2WP_2O_{12}-ZrO_2$  composites with different mass ratios sintered at  $1,200^\circ C$  for 6 h. (A)  $ZrO_2$ , (B) 1:1  $Zr_2WP_2O_{12}:ZrO_2$ , (C) 2:1  $Zr_2WP_2O_{12}:ZrO_2$ , (D) 3:1  $Zr_2WP_2O_{12}:ZrO_2$ , (E) 4:1  $Zr_2WP_2O_{12}-ZrO_2$ , (F)  $Zr_2WP_2O_{12}$ .

## EXPERIMENTAL DETAILS

All  $Zr_2WP_2O_{12}$ ,  $ZrO_2$ , and  $Zr_2WP_2O_{12}/ZrO_2$  ceramics (mass ratios: 1:1, 2:1, 3:1, 4:1) were synthesized through a conventional solid state route. The raw materials were  $ZrO_2$  (Aladdin, purity  $\geq 99.95\%$ ),  $WO_3$  (Aladdin, purity  $\geq 99.95\%$ ), and  $NH_4H_2PO_4$  powders (Aladdin, purity  $\geq 99.5\%$ ). A summary of samples prepared can be found in Table 1. Reactant mixtures were milled for 6 h to form a homogeneous powder and dried at  $80^\circ C$ , followed by heating at  $500^\circ C$  for 3 h. After this pre-sintering step, the mixtures were uni-axially cold pressed into pellets of 7 mm in diameter and about 2 mm in thickness. Pellets were calcined at  $1,200^\circ C$  in air for 6 h and cooled down in the furnace.

Powder X-ray diffraction experiments were performed on a Shimadzu XRD 7000 using  $CuK\alpha$  radiation. Data were collected at 40 kV and 30 mA over the  $10^\circ$  to  $60^\circ$   $2\theta$  range with a scanning speed of  $5^\circ/min$ . The fractured surface morphologies of the samples were observed using a TESCAN VEGA3 scanning electron microscope (SEM). The relative densities of the resulting samples were measured using Archimedes' method. The CTEs of the samples were measured with a Seiko 6300 TMA/SS thermal mechanical analyzer at a heating rate of  $5^\circ C/min$  in air between 25 and  $700^\circ C$ .

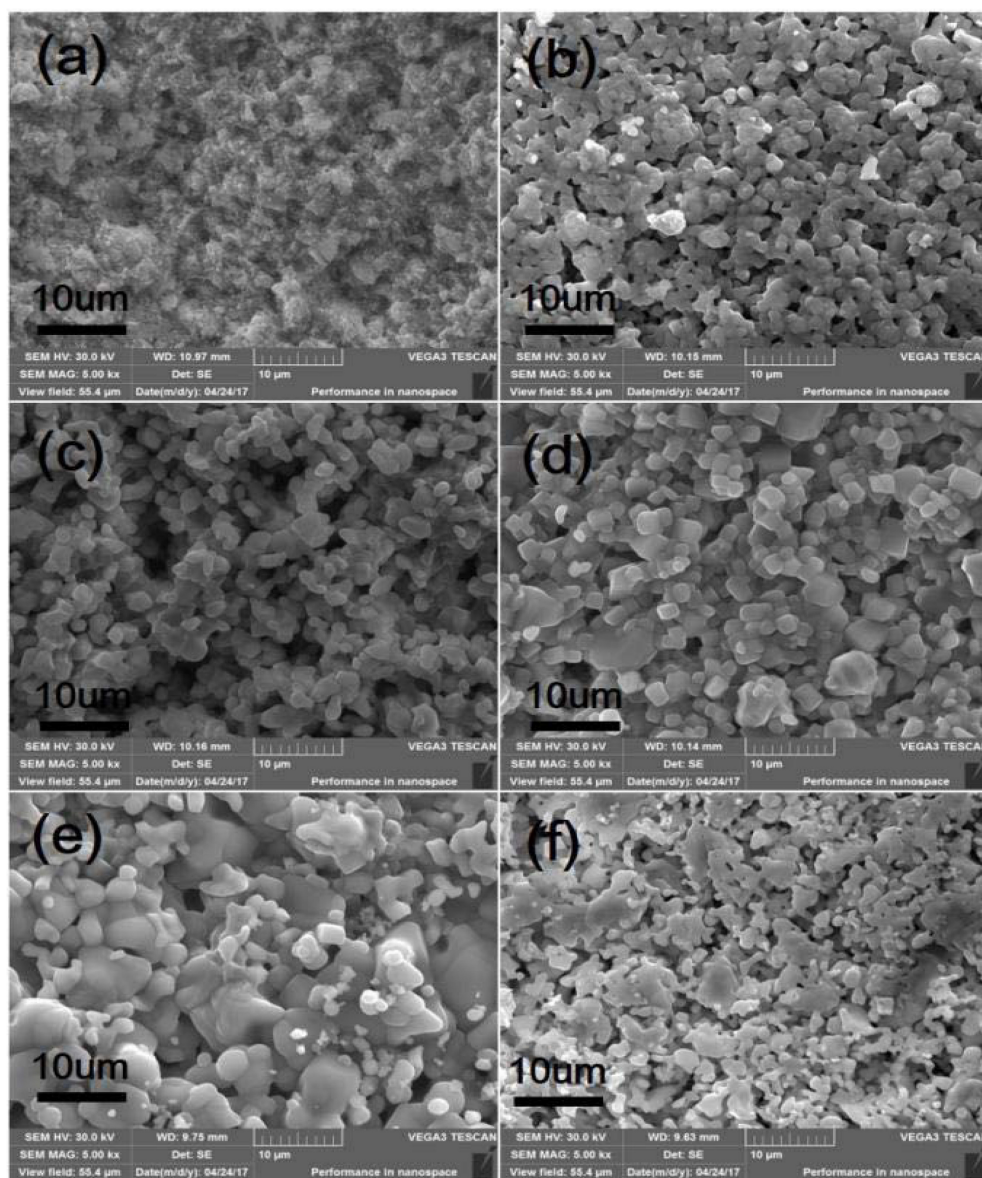


**FIGURE 2** | SEM images of  $ZrO_2$ ,  $Zr_2WP_2O_{12}$ , and  $Zr_2WP_2O_{12}$ - $ZrO_2$  composites with different mass ratios sintered at  $1,200^\circ\text{C}$  for 6 h, (a)  $ZrO_2$ , (b) 1:1  $Zr_2WP_2O_{12}$ : $ZrO_2$ , (c) 2:1  $Zr_2WP_2O_{12}$ : $ZrO_2$ , (d) 3:1  $Zr_2WP_2O_{12}$ : $ZrO_2$ , (e) 4:1  $Zr_2WP_2O_{12}$ : $ZrO_2$ , (f)  $Zr_2WP_2O_{12}$ .

## RESULTS AND DISCUSSION

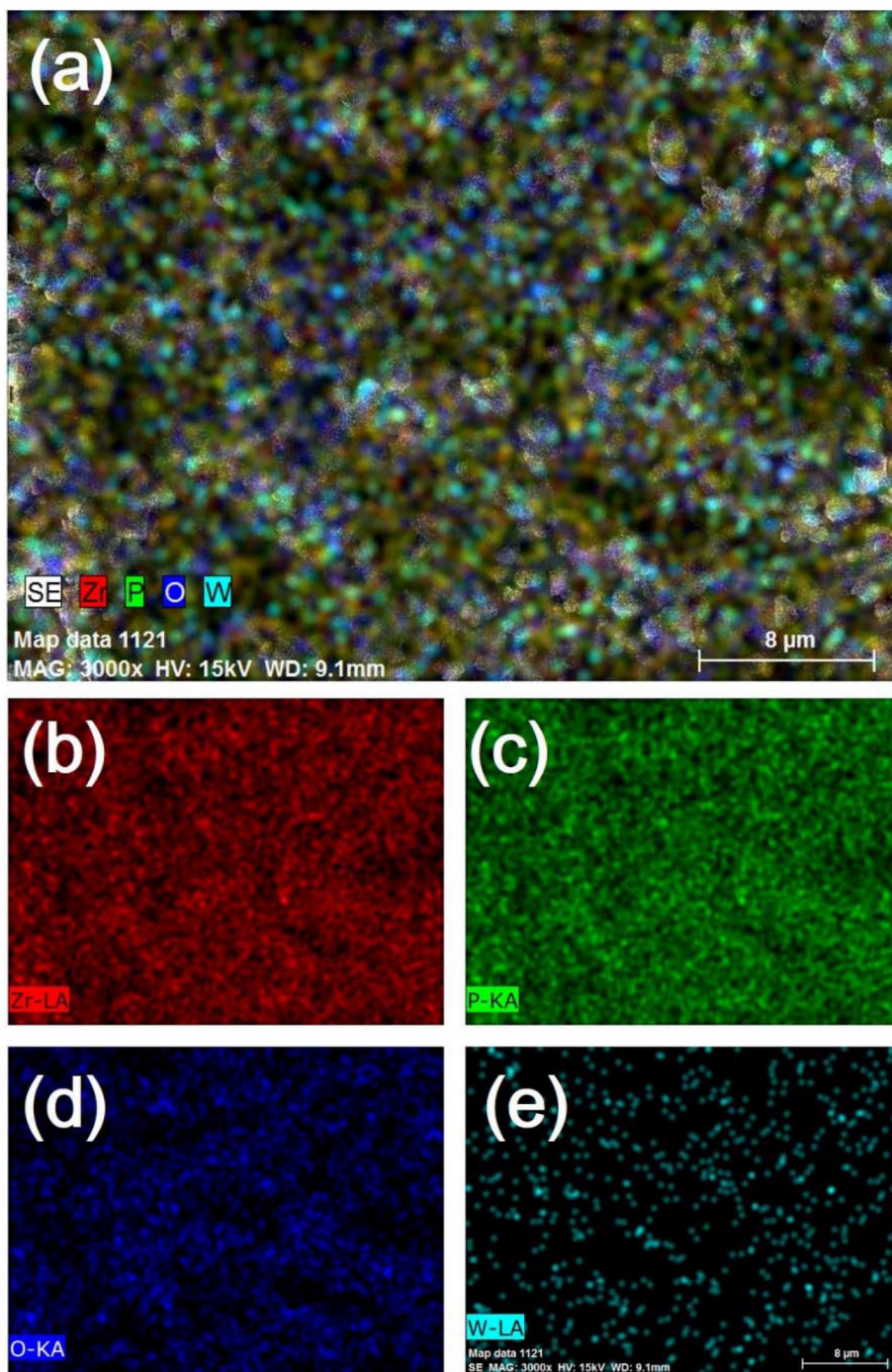
### XRD Analysis

Figure 1 shows typical room temperature XRD patterns of  $Zr_2WP_2O_{12}/ZrO_2$  composites with different mass ratios synthesized at  $1,200^\circ\text{C}$  for 6 h. The XRD patterns of pure  $ZrO_2$  and pure  $Zr_2WP_2O_{12}$  ceramics are also displayed for reference. For pure  $ZrO_2$  ceramics (Figure 1A), all observed reflections could be well indexed and attributed to monoclinic  $ZrO_2$  in agreement with JCPDS card number 65-1,023. For pure  $Zr_2WP_2O_{12}$  ceramics (Figure 1F), all diffraction peaks matched those expected for orthorhombic  $Zr_2WP_2O_{12}$  (JCPDS 43-0258). No impurity phases were detected. XRD patterns of

$Zr_2WP_2O_{12}/ZrO_2$  composites with mass ratios of 1:1, 2:1, 3:1, and 4:1 (Figures 1B–E) displayed diffraction peaks belonging to both monoclinic  $ZrO_2$  and orthorhombic  $Zr_2WP_2O_{12}$ . As no intermediate phase exists between  $ZrO_2$  and  $Zr_2WP_2O_{12}$ , no reaction can occur between excess  $ZrO_2$  and  $Zr_2WP_2O_{12}$ . As expected, the diffraction peaks of  $Zr_2WP_2O_{12}$  became more intense with increasing mass ratio of  $Zr_2WP_2O_{12}$ .

### SEM and Density Analysis

SEM micrographs of different weight ratio  $Zr_2WP_2O_{12}/ZrO_2$  ceramic composites,  $ZrO_2$  and  $Zr_2WP_2O_{12}$  ceramics after sintering at  $1,200^\circ\text{C}$  for 6 h are shown in Figure 2. The SEM



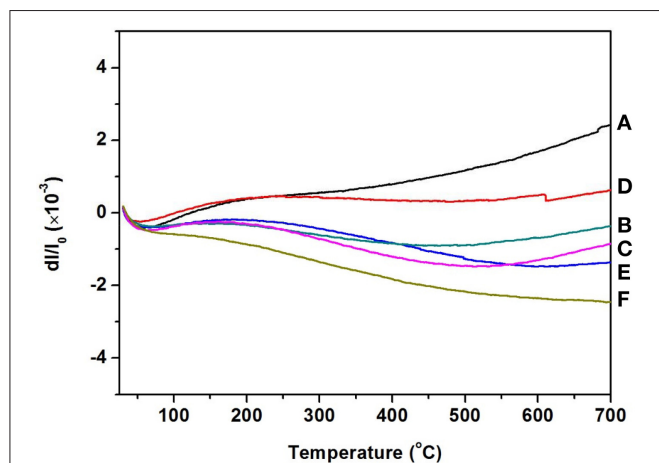
**FIGURE 3** | EDX composition maps (a) Zr, P, W and O, (b) Zr, (c) P, (d) O, and (e) W analysis for 2:1  $Zr_2WP_2O_{12}:ZrO_2$  composite.

image of the  $ZrO_2$  ceramics (**Figure 2a** revealed significant porosity, which is likely due to insufficient sintering. It is known that the sintering temperature required to fabricate dense and tough  $ZrO_2$  ceramics is higher than  $1,400^\circ C$  (Varga et al., 2007). **Figures 2b–e** show SEM images of sintered  $Zr_2WP_2O_{12}/ZrO_2$  ceramic composites as a function of different mass ratios. With

increasing amount of  $Zr_2WP_2O_{12}$ ,  $Zr_2WP_2O_{12}/ZrO_2$  ceramic composites sintered for the same time at the same temperature became denser and displayed larger grain sizes and less porosity. The average grain size of 1:1  $Zr_2WP_2O_{12}/ZrO_2$  composites was about  $2\text{--}3\ \mu m$ , but increased to about  $6\text{--}8\ \mu m$  when the mass ratio of  $Zr_2WP_2O_{12}/ZrO_2$  was increased to 4:1. Pure  $Zr_2WP_2O_{12}$

**TABLE 2** | Relative densities of  $ZrO_2$ ,  $Zr_2WP_2O_{12}$ , and  $Zr_2WP_2O_{12}-ZrO_2$  composites with different mass ratios.

Sample	Relative density (%)
$ZrO_2$	74.5
1:1 $Zr_2WP_2O_{12}-ZrO_2$	84.1
2:1 $Zr_2WP_2O_{12}-ZrO_2$	85.5
3:1 $Zr_2WP_2O_{12}-ZrO_2$	89.8
4:1 $Zr_2WP_2O_{12}-ZrO_2$	91.5
$Zr_2WP_2O_{12}$	79.7

**FIGURE 4** | Thermal expansion curves of  $ZrO_2$ ,  $Zr_2WP_2O_{12}$ , and  $Zr_2WP_2O_{12}-ZrO_2$  composites. (A)  $ZrO_2$ , (B) 1:1  $Zr_2WP_2O_{12}:ZrO_2$ , (C) 2:1  $Zr_2WP_2O_{12}:ZrO_2$ , (D) 3:1  $Zr_2WP_2O_{12}:ZrO_2$ , (E) 4:1  $Zr_2WP_2O_{12}:ZrO_2$ , (F)  $Zr_2WP_2O_{12}$ .**TABLE 3** | Average linear thermal expansion coefficients of  $ZrO_2$ ,  $Zr_2WP_2O_{12}$ , and  $Zr_2WP_2O_{12}-ZrO_2$  composites in corresponding testing temperature range from 25 to 700°C.

Samples	Coefficient of thermal expansion
$ZrO_2$	$4.10 \times 10^{-6} K^{-1}$
1:1 $Zr_2WP_2O_{12}-ZrO_2$	$1.32 \times 10^{-6} K^{-1}$
2:1 $Zr_2WP_2O_{12}-ZrO_2$	$-0.09 \times 10^{-6} K^{-1}$
3:1 $Zr_2WP_2O_{12}-ZrO_2$	$-0.88 \times 10^{-6} K^{-1}$
4:1 $Zr_2WP_2O_{12}-ZrO_2$	$-1.50 \times 10^{-6} K^{-1}$
$Zr_2WP_2O_{12}$	$-3.30 \times 10^{-6} K^{-1}$

(Figure 2f) showed a wide size distribution of spherical grains with some residual porosity, which is in agreement with results reported earlier (Isobe et al., 2008, 2009; Cetinkol and Wilkinson, 2009). Figure 3 shows the composition maps analysis of the 2:1  $Zr_2WP_2O_{12}:ZrO_2$  composite. Homogeneous spatial distributions of Zr, P, W, and O elements were observed. These results indicate that  $Zr_2WP_2O_{12}$  and  $ZrO_2$  phase uniformly distributed as expected.

In this work, the densities of the resulting  $Zr_2WP_2O_{12}$ ,  $ZrO_2$ , and  $Zr_2WP_2O_{12}/ZrO_2$  (mass ratio: 1:1, 2:1, 3:1, 4:1) ceramics were also measured using Archimedes' technique. The relative densities were calculated from theoretical values for  $Zr_2WP_2O_{12}$

( $3.63 \text{ g/cm}^3$ ) and  $ZrO_2$  ( $5.817 \text{ g/cm}^3$ ). As shown in Table 2, the results are consistent with the SEM analysis above. The relative densities of pure  $Zr_2WP_2O_{12}$  and  $ZrO_2$  were low, however, the densities of  $Zr_2WP_2O_{12}/ZrO_2$  (mass ratio: 1:1, 2:1, 3:1, 4:1) ceramics increased with increasing content of  $Zr_2WP_2O_{12}$ . For a 4:1 mass ratio  $Zr_2WP_2O_{12}/ZrO_2$  composite, the relative density of the sample reached 91.5% of the theoretical density values. The sintering temperature of  $Zr_2WP_2O_{12}$  is lower than that of  $ZrO_2$ , which results in a decreased sintering temperature and better densification of  $Zr_2WP_2O_{12}/ZrO_2$  ceramics with increasing content of  $Zr_2WP_2O_{12}$ .

## Thermal Expansion Analysis

Figure 4 gives the information about the thermal expansion of all the  $Zr_2WP_2O_{12}/ZrO_2$  ceramic composites synthesized at 1,200°C for 6 h. For purposes of comparison, the thermal expansion curves of pure  $ZrO_2$  and pure  $Zr_2WP_2O_{12}$  ceramics are also given in Figure 4. Average linear CTEs of the obtained  $ZrO_2$ ,  $Zr_2WP_2O_{12}$ , and  $Zr_2WP_2O_{12}/ZrO_2$  ceramics with different mass ratios are summarized in Table 3. Pure  $ZrO_2$  ceramics (Figure 4A) showed positive thermal expansion between 25 and 700°C, and the average linear CTE was measured to be  $4.1 \times 10^{-6} K^{-1}$ , which is lower than the value reported in the literature (Lommens et al., 2005; Yang et al., 2007). This is likely due to insufficient sintering of the  $ZrO_2$  ceramics, as some of the expansion can be absorbed by the empty pore space. Pure  $Zr_2WP_2O_{12}$  ceramics (Figure 4F) showed NTE in the testing temperature range. The average linear CTE of the  $Zr_2WP_2O_{12}$  ceramics was measured to be  $-3.3 \times 10^{-6} K^{-1}$  in the temperature range of 25–700°C, which is consistent with literature reports (Cetinkol and Wilkinson, 2009; Isobe et al., 2009). As can be expected, the CTEs of the  $Zr_2WP_2O_{12}/ZrO_2$  composites decreased from  $4.1 \times 10^{-6} K^{-1}$  to  $-3.3 \times 10^{-6} K^{-1}$  as the weight fraction of  $Zr_2WP_2O_{12}$  was increased. As shown in Figure 4C, the 2:1  $Zr_2WP_2O_{12}/ZrO_2$  specimen showed close to zero thermal expansion with an average linear CTE of  $-0.09 \times 10^{-6} K^{-1}$  in the temperature range of 25–700°C. This near zero expansion ceramic composite will have a number of potential applications in many fields. These results suggest that the CTE of the  $Zr_2WP_2O_{12}-ZrO_2$  composites can be modified in the range from  $4.1 \times 10^{-6} K^{-1}$  to  $-3.3 \times 10^{-6} K^{-1}$ , and that it is even possible to achieve zero thermal expansion by adjusting the mass ratios of  $Zr_2WP_2O_{12}$  and  $ZrO_2$ .

## CONCLUSIONS

$Zr_2WP_2O_{12}/ZrO_2$  ceramic composites with adjustable thermal expansion coefficients were successfully fabricated by a solid state reaction method. The composites consisted of orthorhombic  $Zr_2WP_2O_{12}$  and monoclinic  $ZrO_2$  with no intermediate phases observed. With increasing amount of  $Zr_2WP_2O_{12}$ , the relative densities of the  $Zr_2WP_2O_{12}/ZrO_2$  ceramic composites increased gradually. The CTE of the  $Zr_2WP_2O_{12}/ZrO_2$  composites can be tailored from  $4.1 \times 10^{-6} K^{-1}$  to  $-3.3 \times 10^{-6} K^{-1}$  by changing the weight fraction of  $Zr_2WP_2O_{12}$ . For a mass ratio of  $Zr_2WP_2O_{12}/ZrO_2$  of 2:1, the  $Zr_2WP_2O_{12}/ZrO_2$  ceramic

composite showed close to zero thermal expansion with an average linear CTE of  $-0.09 \times 10^{-6} \text{ K}^{-1}$  between 25 and  $700^\circ\text{C}$ .

## AUTHOR CONTRIBUTIONS

HL, XC, and ZZ designed experiments; WS and GX carried out experiments; HL, ZZ, and XZ analyzed experimental results and wrote the manuscript.

## REFERENCES

- Banek, N. A., Baiz, H. I., Latigo, A., and Lind, C. (2010). Autohydration of nanosized cubic zirconium tungstate. *J. Am. Chem. Soc.* 132, 8278–8279. doi: 10.1021/ja101475f
- Cetinkol, M., and Wilkinson, A. P. (2009). Pressure dependence of negative thermal expansion in  $Zr_2(WO_4)(PO_4)_2$ . *Solid State Commun.* 149, 421–424. doi: 10.1016/j.ssc.2009.01.002
- De Buysser, K., Lommens, P., De Meyer, C., Bruneel, E., Hoste, S., and Driessche, I. V. (2004).  $ZrO_2$ - $ZrW_2O_8$  composites with tailor-made thermal expansion. *Ceram. Silikaty* 48, 139–144.
- Gao, X., Coleman, M. R., and Lind, C. (2016). Surface modification of  $ZrW_2O_8$  and  $ZrW_2O_7(OH)_2 \cdot 2H_2O$  filler particles for controlled thermal expansion polycarbonate composites. *Pol. Comp.* 37, 1359–1368. doi: 10.1002/pc.23304
- Hu, L., Chen, J., Fan, L. L., Ren, Y., Rong, Y. C., Pan, Z., et al. (2014). Zero thermal expansion and ferromagnetism in cubic  $Sc_{1-x}M_xF_3$  ( $M = Ga, Fe$ ) over a wide temperature range. *J. Am. Chem. Soc.* 136, 13566–13569. doi: 10.1021/ja5077487
- Isobe, T., Kato, Y., Mizutani, M., Ota, T., and Daimon, K. (2008). Pressureless sintering of negative thermal expansion  $ZrW_2O_8/Zr_2WP_2O_{12}$  composites. *Mater. Lett.* 62, 3913–3915. doi: 10.1016/j.matlet.2008.05.046
- Isobe, T., Umezome, T., Kameshima, Y., Nakajima, A., and Okada, K. (2009). Preparation and properties of negative thermal expansion  $Zr_2WP_2O_{12}$  ceramics. *Mater. Res. Bull.* 44, 2045–2049. doi: 10.1016/j.materresbull.2009.07.020
- Khazeni, N., Mavis, B., Gunduz, G., and Colak, U. (2011). Synthesis of zirconium tungstate-zirconia core-shell composite particles. *Mater. Res. Bull.* 46, 2025–2031. doi: 10.1016/j.materresbull.2011.07.006
- Liu, H. F., Pan, K. M., Jin, Q., Zhang, Z. P., Wang, G., and Zeng, X. H. (2014). Negative thermal expansion and shift in phase transition temperature in Mo-substituted  $ZrW_2O_8$  thin films prepared by pulsed laser deposition. *Ceram. Int.* 40, 3873–3878. doi: 10.1016/j.ceramint.2013.08.028
- Liu, H. F., Zhang, W., Zhang, Z. P., and Chen, X. B. (2012). Synthesis and negative thermal expansion properties of solid solutions  $Yb_{2-x}La_xW_3O_{12}$  ( $0 \leq x \leq 2$ ). *Ceram. Int.* 38, 2951–2956. doi: 10.1016/j.ceramint.2011.11.072
- Liu, H. F., Zhang, Z. P., Ma, J., Zhu, J., and Zeng, X. H. (2015). Effect of isovalent substitution on phase transition and negative thermal expansion of  $In_{2-x}Sc_xW_3O_{12}$  ceramics. *Ceram. Int.* 41, 9873–9877. doi: 10.1016/j.ceramint.2015.04.062
- Liu, Q. Q., Yang, J., Cheng, X. N., Liang, G. S., and Sun, X. J. (2012). Preparation and characterization of negative thermal expansion  $Sc_2W_3O_{12}/Cu$  core-shell composite. *Ceram. Int.* 38, 541–545. doi: 10.1016/j.ceramint.2011.07.041
- Lommens, P., Meyer, C. D., Bruneel, E., Buysser, K. D., Driessche, I. V., and Hoste, S. (2005). Synthesis and thermal expansion of  $ZrO_2/ZrW_2O_8$  composites. *J. Eur. Ceram. Soc.* 25, 3605–3610. doi: 10.1016/j.jeurceramsoc.2004.09.015
- Mary, T. A., Evans, J. S. O., Vogt, T., and Sleight, A. W. (1996). Negative thermal expansion from 0.3 K to 1050 K in  $ZrW_2O_8$ . *Science* 272, 90–92. doi: 10.1126/science.272.5258.90

## ACKNOWLEDGMENTS

The authors thank the National Natural Science Foundation of China (No.51602280 and No.51102207), Qing Lan Project of Jiangsu Province, Guang ling College of Yangzhou University Natural Science Research Foundation (No. ZKZD17001). The authors are grateful to Dr. Cora Lind-Kovacs for revising the paper.

- Miao, X. G., Sun, D., Hoo, P. W., Liu, J. L., Hu, Y. F., and Chen, Y. M. (2004). Effect of titania addition on yttria-stabilised tetragonal zirconia ceramics sintered at high temperatures. *Ceram. Int.* 30, 1041–1047. doi: 10.1016/j.ceramint.2003.10.025
- Perottoni, C. A., and Jornada, J. A. H. (1998). Pressure-induced amorphization and negative thermal expansion in  $ZrW_2O_8$ . *Science* 280, 886–888. doi: 10.1126/science.280.5365.886
- Romao, C. P., Marinkovic, B. A., Werner-Zwanzige, U., and White, M. A. (2015). Thermal expansion reduction in alumina-toughened zirconia by incorporation of zirconium tungstate and aluminum tungstate. *J. Am. Chem. Soc.* 98, 2858–2865. doi: 10.1111/jace.13675
- Sullivan, L. M., and Lukehart, C. M. (2005). Zirconium tungstate ( $ZrW_2O_8$ )/polyimide nanocomposites exhibiting reduced coefficient of thermal expansion. *Chem. Mater.* 17, 2136–2141. doi: 10.1021/cm0482737
- Sumithra, S., and Umarji, A. M. (2004). Role of crystal structure on the thermal expansion of  $Ln_2W_3O_{12}$  ( $Ln = La, Nd, Dy, Y, Er$  and  $Yb$ ). *Solid State Sci.* 6, 1313–1319. doi: 10.1016/j.solidstatesciences.2004.07.023
- Sumithra, S., and Umarji, A. M. (2006). Negative thermal expansion in rare earth molybdates. *Solid State Sci.* 8, 1453–1458. doi: 10.1016/j.solidstatesciences.2006.03.010
- Tani, J., Takahashi, M., and Kido, H. (2010). Fabrication and thermal expansion properties of  $ZrW_2O_8/Zr_2WP_2O_{12}$  composites. *J. Eur. Ceram. Soc.* 30, 1483–1488. doi: 10.1016/j.jeurceramsoc.2009.11.010
- Varga, T., Lind, C., Wilkinson, A. P., Xu, H., Leshner, C. E., and Navrotsky, A. (2007). Heats of formation for several crystalline polymorphs and pressure-induced amorphous forms of  $AMo_2O_8$  ( $A = Zr, Hf$ ) and  $ZrW_2O_8$ . *Chem. Mater.* 19, 468–476. doi: 10.1021/cm0617743
- Yang, J., Yang, Y. S., Liu, Q. Q., Xu, G. F., and Cheng, X. N. (2010). Preparation of negative thermal expansion  $ZrW_2O_8$  powders and its application in polyimide/ $ZrW_2O_8$  composites. *J. Mater. Sci. Technol.* 26, 665–668. doi: 10.1016/S1005-0302(10)60103-X
- Yang, X. B., Cheng, X. N., Yan, X. H., Yang, J., Fu, T. B., and Qiu, J. (2007). Synthesis of  $ZrO_2/ZrW_2O_8$  composites with low thermal expansion. *Compos. Sci. Technol.* 67, 1167–1171. doi: 10.1016/j.compscitech.2006.05.012
- Yilmaz, S. (2002). Thermal mismatch stress development in  $Cu-ZrW_2O_8$  composite investigated by synchrotron X-ray diffraction. *Comp. Sci. Technol.* 62, 1835–1839. doi: 10.1016/S0266-3538(02)00104-5

**Conflict of Interest Statement:** The authors declare that the research was conducted in the absence of any commercial or financial relationships that could be construed as a potential conflict of interest.

Copyright © 2017 Zhang, Sun, Liu, Xie, Chen and Zeng. This is an open-access article distributed under the terms of the Creative Commons Attribution License (CC BY). The use, distribution or reproduction in other forums is permitted, provided the original author(s) or licensor are credited and that the original publication in this journal is cited, in accordance with accepted academic practice. No use, distribution or reproduction is permitted which does not comply with these terms.